arXiv:1003.0539v2 [cond-mat.supr-con] 19 Mar 2010

Magnetic excitations of $Fe_{1+y}Se_xTe_{1-x}$ in magnetic and superconductive phases

P. Babkevich[1,2], M. Bendele[3,4], A. T. Boothroyd[1], K. Conder[5], S. N. Gvasaliya[2], R. Khasanov[3], E. Pomjakushina[5] and B. Roessli[2]

1 Department of Physics, Clarendon Laboratory, Oxford University, Oxford OX1 3PU, United Kingdom

2 Laboratory for Neutron Scattering, Paul Scherrer Institut, CH-5232 Villigen PSI, Switzerland

[3] Laboratory for Muon Spin Spectroscopy, Paul Scherrer Institut, CH-5232 Villigen PSI, Switzerland

[4] Physik-Institut der Universität Zürich, Winterthurerstrasse 190, CH-8057 Zürich, Switzerland

[5] Laboratory for Developments and Methods, Paul Scherrer Institut, CH-5232 Villigen PSI, Switzerland

E-mail: peter.babkevich@physics.ox.ac.uk

PACS numbers: 74.70.Xa, 76.50.+g, 61.05.F-, 76.75.+i

Abstract. We have used inelastic neutron scattering and muon-spin rotation to compare the low energy magnetic excitations in single crystals of superconducting $Fe_{1.01}Se_{0.50}Te_{0.50}$ and non-superconducting $Fe_{1.10}Se_{0.25}Te_{0.75}$. We confirm the existence of a spin resonance in the superconducting phase of $Fe_{1.01}Se_{0.50}Te_{0.50}$, at an energy of 7 meV and a wavevector of $(1/2, 1/2, 0)$. The non-superconducting sample exhibits two incommensurate magnetic excitations at $(1/2, 1/2, 0) \pm (0.18, -0.18, 0)$ which rise steeply in energy, but no resonance is observed at low energies. A strongly dispersive low-energy magnetic excitation is also observed in $Fe_{1.10}Se_{0.25}Te_{0.75}$ close to the commensurate antiferromagnetic ordering wavevector $(1/2 - \delta, 0, 1/2)$ where $\delta \approx 0.03$. The magnetic correlations in both samples are found to be quasi-two dimensional in character and persist well above the magnetic ($Fe_{1.10}Se_{0.25}Te_{0.75}$) and superconducting ($Fe_{1.01}Se_{0.50}Te_{0.50}$) transition temperatures.

1. Introduction

Considerable effort has been devoted over the past two years to investigate the basic properties of the Fe-based family of superconductors [1, 2, 3]. A central question is whether magnetism plays an important role in the formation of the superconducting state. A useful strategy to tackle this problem is to combine neutron scattering and muon spin rotation (μSR) measurements on one and the same sample. Neutron scattering provides information on magnetic correlations and on the nature of the magnetic excitations, while μSR can determine whether static magnetic order and/or bulk superconductivity exists.

The $Fe_{1+y}Se_xTe_{1-x}$ system is a convenient one to study with this methodology as large high-quality crystals can be grown [4, 5] and the tetragonal crystallographic structure is relatively simple to analyse and model. Single crystals are easier to grow if there is a small excess of Fe (i.e. $y > 0$), especially for small x [6, 7, 8, 9].

The pure FeSe compound is a superconductor with a transition temperature $T_c \sim 8\,\mathrm{K}$ [6]. The T_c can be increased by partial substitution of Te for Se such that $T_c \sim 14\,\mathrm{K}$ for $0.4 \lesssim x \lesssim 0.8$ and $y \approx 0$ [10, 11]. The application of pressure has also been found to raise T_c, with values as high as 37 K observed for FeSe [12, 13, 14, 15]. Compounds with $x \lesssim 0.4$ do not exhibit bulk superconductivity but order magnetically below a temperature which has a maximum of 67 K at $x = 0$ and which decreases with x and vanishes at $x \sim 0.4$. We recently found evidence for coexistence of incommensurate magnetic order and partial superconductivity for $x \sim 0.25$ [11].

In this study, we present neutron scattering and μSR measurements on two single crystal samples: (i) $Fe_{1.01}Se_{0.50}Te_{0.50}$, a bulk superconductor, and (ii) $Fe_{1.10}Se_{0.25}Te_{0.75}$, a non-superconducting sample which exhibits magnetic order. In superconducting $Fe_{1.01}Se_{0.50}Te_{0.50}$ we observe a resonant magnetic excitation consistent with that reported previously in compounds with similar compositions [16, 17, 18, 19]. In $Fe_{1.10}Se_{0.25}Te_{0.75}$ we observe strongly dispersive, low energy magnetic excitations associated with the magnetic ordering wavevector $(1/2 - \delta, 0, 1/2)$, $\delta \approx 0.03$, and also with the wavevectors $(1/2, 1/2, 0) \pm (0.18, -0.18, 0)$. We find no evidence for a resonance peak in the excitation spectrum of $Fe_{1.10}Se_{0.25}Te_{0.75}$.

2. Experimental Details

Single crystals of $Fe_{1+y}Se_xTe_{1-x}$ were grown by a modified Bridgman method as reported by [4]. Neutron scattering measurements were carried out on triple-axis spectrometer TASP [20] at the SINQ [21] spallation source (Paul Scherrer Institut, Switzerland). Bragg reflections from pyrolytic graphite PG(002) monochromator and analyser were used at a fixed final wavevector of $2.66\,\mathrm{Å}^{-1}$. A PG filter was placed after the sample to reduce contamination from higher order harmonics in the beam and the instrument was set up in the open – open – open – open collimation with the analyser focusing in the horizontal plane. The crystals were single rods with masses of approximately 4 g.

The $Fe_{1.10}Se_{0.25}Te_{0.75}$ sample was orientated in two settings to give access to $(h, 0, l)$ and $(h, k, 0)$ planes in reciprocal space. Measurements of $Fe_{1.01}Se_{0.50}Te_{0.50}$ were made in the $(h, k, 0)$ plane only. In this report we index the reciprocal lattice with respect to the primitive tetragonal unit cell described by the $P4/nmm$ space group with unit cell parameters $a \approx 3.8$ Å and $c \approx 6.1$ Å along lines joining the nearest neighbour Fe atoms.

Zero-field-cooled magnetisation measurements were performed on a Quantum Design MPMS magnetometer with a measuring field $\mu_0 H = 0.3$ mT using the direct current method. To reduce the effects of demagnetisation, thin plate-like pieces of $Fe_{1+y}Se_xTe_{1-x}$, cleaved from the main single crystals, were oriented with the flat surface (*ab* plane) parallel to the applied field.

Zero-field (ZF) and transverse-field (TF) muon-spin rotation (μSR) experiments were performed on the πM3 beam line at SμS (Paul Scherrer Institut, Switzerland). In TF experiments a magnetic field of 11.8 mT was applied parallel to the crystallographic *ab* plane of the crystal and perpendicular to the muon-spin polarisation.

3. Results

3.1. Magnetisation and μSR Measurements

Zero-field-cooled magnetisation data normalised to the ideal $1/4\pi$ value ($M_{\rm norm}$) are shown in figure 1(a). The $Fe_{1.01}Se_{0.50}Te_{0.50}$ sample is seen to be a bulk superconductor with the onset of the transition $T_{\rm c}^{\rm onset} \simeq 14.0$ K and $M_{\rm norm} \simeq -0.8$ at $T \simeq 2$ K. The $Fe_{1.10}Se_{0.25}Te_{0.75}$ sample also exhibits superconductivity ($T_{\rm c}^{\rm onset} \simeq 8.6$ K) but has a small superconducting fraction of order 10% at low temperature.

For the $x = 0.5$ sample, the ZF time-spectra measured at $T = 1.7$ K and 20 K are almost identical thus suggesting that the magnetic state of this sample is the same above and below the superconducting transition temperature. The solid lines correspond to a fit by the function $A^{\rm ZF}(t) = A_0^{\rm ZF} e^{-\Lambda^{\rm ZF} t}$, where $A_0^{\rm ZF}$ is the initial asymmetry and $\Lambda^{\rm ZF}$ is the exponential relaxation rate. Such behavior is consistent with dilute Fe moments as observed recently for $FeSe_{1-x}$ [22]. The TF data for $x = 0.5$ fit well to the function $A^{\rm TF}(t) = A_0^{\rm TF} e^{-(\Lambda^{\rm TF} t + \sigma^2 t^2)} \cos(\gamma_\mu B t + \phi)$. Here, $\gamma_\mu/2\pi = 135.5$ MHz/T is the muon gyromagnetic ratio, ϕ is the initial phase of the muon-spin ensemble, and σ is the Gaussian relaxation rate. Figure 1(b) shows that the TF asymmetry $A_0^{\rm TF}$ is almost temperature independent. The slightly stronger relaxation of the muon-spin polarisation at 1.7 K relative to 20 K is due to formation of the vortex lattice at $T < T_{\rm c}$.

Static (within the μSR time window) magnetism develops in $Fe_{1.10}Se_{0.25}Te_{0.75}$ as signalled by a fast drop of both $A^{\rm ZF}$ and $A^{\rm TF}$ within the first 100 ns (see upper panel of figure 1(b)). The solid lines correspond to fits with $A^{\rm ZF}(t) = A_1^{\rm ZF} e^{-\Lambda_1^{\rm ZF} t} + A_2^{\rm ZF} e^{-\Lambda_2^{\rm ZF} t}$ and $A^{\rm TF}(t) = e^{-\sigma^2 t^2/2}[A_1^{\rm TF} e^{-\Lambda_1^{\rm TF} t} \cos(\gamma_\mu B_1 t + \phi) + A_2^{\rm TF} e^{-\Lambda_2^{\rm TF} t} \cos(\gamma_\mu B_2 t + \phi)]$. Here, $A_{1(2)}^{\rm ZF(TF)}$ and $\Lambda_{1(2)}^{\rm ZF(TF)}$ are the initial ZF (TF) asymmetry and the exponential depolarisation rate of the slow (fast) relaxing component, respectively. The temperature evolution of $A_1^{\rm TF}$, shown in figure 1(b), reveals that below 20 K magnetism occupies more than 95% of

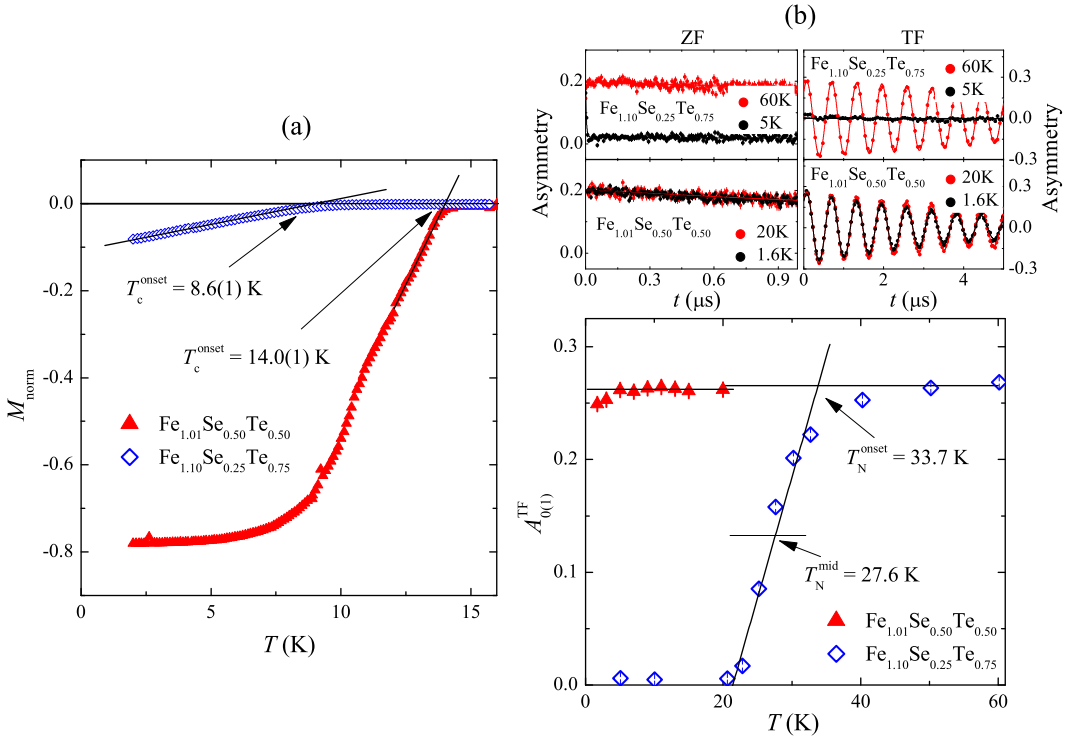


Figure 1. (a) Temperature dependence of the zero-field-cooled magnetisation of $Fe_{1.01}Se_{0.50}Te_{0.50}$ and $Fe_{1.10}Se_{0.25}Te_{0.75}$normalised to the ideal $1/4\pi$ value. The onset T_c^{onset} of the superconducting transition is determined from the intersection of straight lines fit to the data above and below the transition. (b) Representative ZF and TF μSR time spectra (upper plots) and temperature-dependent initial TF asymmetry of the slow relaxing component (A_0^{TF} and A_1^{TF}, lower plot) for single crystals of $Fe_{1.01}Se_{0.50}Te_{0.50}$ and $Fe_{1.10}Se_{0.25}Te_{0.75}$. The onset ($T_N^{onset}$) and the mid-point ($T_N^{mid}$) of the magnetic transition are determined from the intersection of straight lines fit to the data above and below the transition and as the point where the asymmetry decreases by a factor of 2 from its maximum value, respectively.

the whole sample volume. The corresponding values of the onset and the mid-point of the magnetic transitions, determined as shown in the figure, are $T_N^{onset} \simeq 33.7\,K$ and $T_N^{mid} \simeq 27.6\,K$. We note that although the magnetic order is shown to extend throughout virtually the entire volume of the sample, μSR cannot determine whether the magnetic order is long range. The neutron diffraction data presented in the next section show that the magnetic order is in fact relatively short range.

3.2. Neutron Scattering Results

Elastic neutron scattering measurements on $Fe_{1.10}Se_{0.25}Te_{0.75}$ in the $(h, 0, l)$ scattering plane at 2 K, as shown in figure 2(a), reveal a diffuse magnetic peak centred on $(1/2 - \delta, 0, 1/2)$ with $\delta \approx 0.03$. The incommensurate peak is much broader than the resolution of the instrument. From $\boldsymbol{Q}$ scans through the peak we obtain correlation

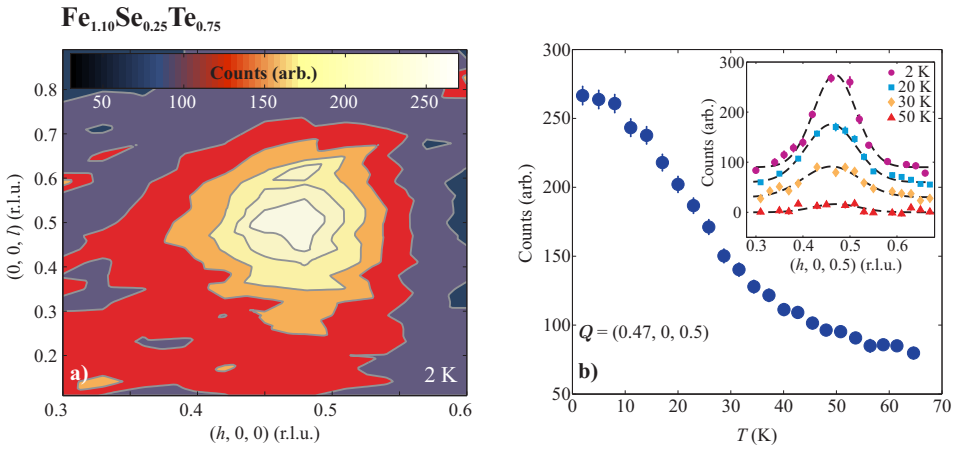


Figure 2. Elastic neutron measurements of $Fe_{1.10}Se_{0.25}Te_{0.75}$ at the magnetic order propagation vector $\boldsymbol{q} = (0.47, 0, 0.5)$. (a) Map showing the incommensurate peak at $\boldsymbol{q}$ in the $(h, 0, l)$ plane at 2 K. (b) Temperature dependence of the intensity at $\boldsymbol{q}$. Inset shows scans along $(h, 0, 0.5)$ measured at 2, 20, 30 and 50 K. A sloping background function has been subtracted from the data and the dashed lines show a Gaussian fit through the peaks. For clarity, the scans have been displaced vertically.

lengths along a and c axes of 11.4(6) Å and 7.5(4) Å respectively at 2 K. Figure 2(b) shows that the magnetic peak develops below $T_N \sim 50$ K. The correlation lengths did not change measurably upon warming through the T_N (figure 2(b): inset). The magnetic propagation vector $\boldsymbol{q} = (1/2 - \delta, 0, \pm 1/2)$ is similar to that found previously for the similar composition $Fe_{1.03}Se_{0.25}Te_{0.75}$ compound. For the latter compound we confirmed that the peak described by $\boldsymbol{q}$ is magnetic in character using neutron polarisation analysis [11]. Our results are consistent with measurements on $Fe_{1.07}Se_{0.25}Te_{0.75}$ for which the incommensurability is found to be $\delta \approx 0.04$ [23].

The magnetic scattering cross-section is directly proportional to the magnetic response function $S(\boldsymbol{Q}, E)$ – the Fourier transform of the space- and time-dependent spin–spin correlation function. According to the fluctuation–dissipation theorem, $S(\boldsymbol{Q}, E)$ is in turn related to the imaginary part of the dynamical susceptibility $\chi''(\boldsymbol{Q}, E)$ by [24]

$$S(\boldsymbol{Q}, E) = \frac{1}{\pi} \left[n(E, T) + 1 \right] \chi''(\boldsymbol{Q}, E). \tag{1}$$

The Bose–Einstein population factor $n(E, T) = [\exp(E/k_B T) - 1]^{-1}$ (where k_B is the Boltzmann constant) takes into account the increase in scattering from bosonic excitations due to thermal population at temperatures $T > 0$. Correction for this factor allows the temperature dependence of $\chi''(\boldsymbol{Q}, E)$ to be studied.

Figure 3(a) shows background corrected scans along the $(h, 0, 0.6)$ direction at energy transfers of 2, 4 and 6 meV for the $Fe_{1.10}Se_{0.25}Te_{0.75}$ crystal. A peak at $\boldsymbol{Q} = \boldsymbol{q}$ is present in each scan, indicating a strongly dispersing excitation. The broadening of the dispersion in $\boldsymbol{Q}$ may be due to unresolvable splitting of the mode into two excitations at higher energies. The measured magnetic response at 2 meV parallel to

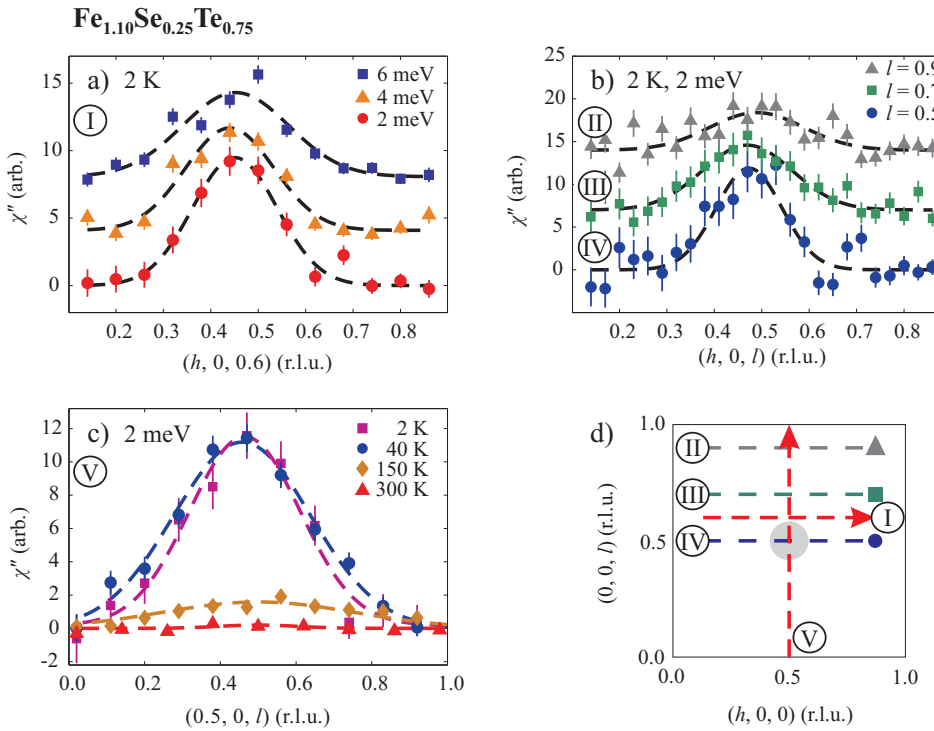


Figure 3. Inelastic neutron scattering from $Fe_{1.10}Se_{0.25}Te_{0.75}$ in the vicinity of the magnetic ordering wavevector $\boldsymbol{q} = (0.47, 0, 0.5)$. (a) Constant energy scans collected at 2, 4 and 6 meV and 2 K along $(h, 0, 0.6)$. The data has been shifted in $\chi''(\boldsymbol{Q}, E)$ by arbitrary amounts for clarity. (b) Constant energy scans collected at 2 meV and temperature of 2 K showing $\chi''(\boldsymbol{Q}, E)$ along $(h, 0, 0.5)$, $(h, 0, 0.7)$ and $(h, 0, 0.9)$. The plots have been displaced and the dashed lines show Gaussian peaks through the spectra. (c) Constant energy scans at 2 meV at temperatures of 2, 40, 150 and 300 K showing $\chi''(\boldsymbol{Q}, E)$ along $(0.5, 0, l)$. Note that a linear background has been subtracted in all scans. (d) Diagram of the $(h, 0, l)$ plane to show scan directions denoted by roman numerals.

$(1, 0, 0)$ for $l = 0.5$, 0.7 and 0.9, as shown in figure 3(b), reveals considerable broadening of $\chi''(\boldsymbol{Q}, E)$ in the out-of-plane direction. Such broadening is characteristic of a quasi-two-dimensional system with weak interactions along c. Figure 3(c) shows that spin fluctuations persist up to at least 150 K, well into the paramagnetic state. At 40 K, i.e. close to the magnetic ordering temperature, $\chi''(\boldsymbol{Q}, E)$ is almost the same as at 2 K.

We now turn to the low energy excitation spectrum in the vicinity of the wavevector $(1/2, 1/2, 0)$. Figures 4(a) and (b) show maps of $\chi''(\boldsymbol{Q}, E)$ measured along $(h, 1-h, 0)$ for $Fe_{1.10}Se_{0.25}Te_{0.75}$ at 2 and 40 K. The fluctuations measured at 2 K are consistent with the magnetic excitation spectrum at higher energies reported for $Fe_{1.03}Se_{0.27}Te_{0.73}$ [25]. The excitation spectrum at 2 K is characterised by steep incommensurate branches arising from $(1/2 \pm \epsilon, 1/2 \mp \epsilon, 0)$ where $\epsilon \approx 0.18$. The incommensurate excitation are still present at 40 K. The scans shown in figure 4(c) reveal that at $E = 7$ meV, the system response is nearly the same at 2 K as at 40 K. The background corrected $\chi''(\boldsymbol{Q}, E)$ for the $Fe_{1.10}Se_{0.25}Te_{0.75}$ sample does not appear to change for energies in the 2 to 7 meV

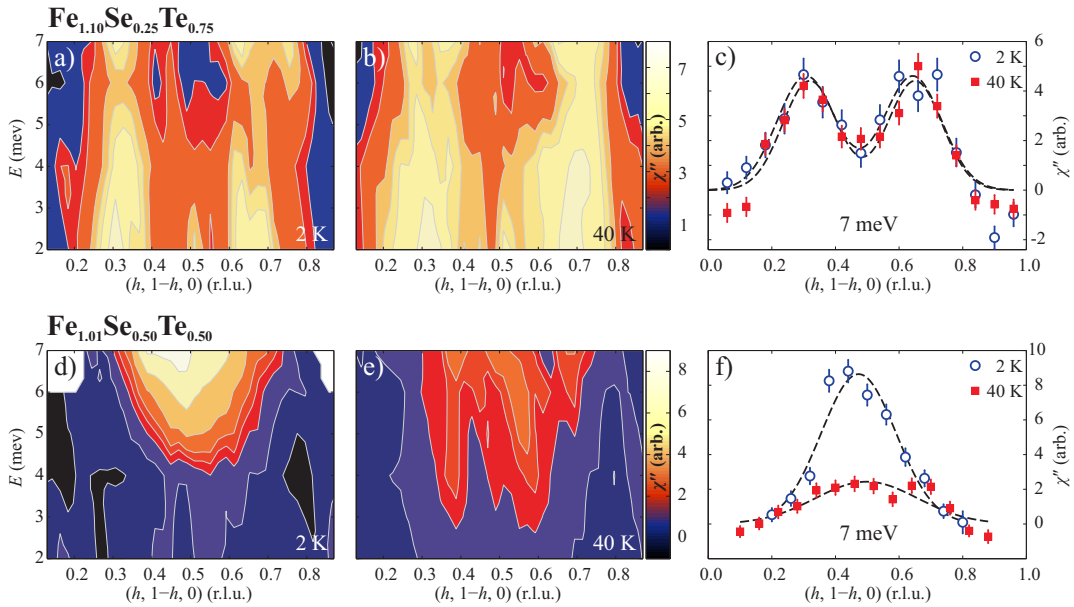


Figure 4. Variation of $\chi''(\boldsymbol{Q}, E)$ in the $(h, 1-h, 0)$ direction for energies between 2 meV and 7 meV at temperatures of 2 and 40 K. Data in (a)–(c) are from $Fe_{1.10}Se_{0.25}Te_{0.75}$ and in (d)–(f) are from $Fe_{1.01}Se_{0.50}Te_{0.50}$. Constant energy cuts at 7 meV along $(h, 1-h, 0)$, measured at 2 and 40 K for $Fe_{1.10}Se_{0.25}Te_{0.75}$ and $Fe_{1.01}Se_{0.50}Te_{0.50}$ are shown in (c) and (f) respectively. A flat background has been subtracted in all scans and dashed lines through the data are fits with a Gaussian lineshape.

range measured at these temperatures. This is also the case for measurements along $(1/2, 0, l)$ in figure 3(c) that show $\chi''(\boldsymbol{Q}, E)$ data at 2 meV to be similar at 2 and 40 K.

The results obtained for $Fe_{1.01}Se_{0.50}Te_{0.50}$ are in stark contrast to those of the non-superconducting $Fe_{1.10}Se_{0.25}Te_{0.75}$ sample just described. Figures 4(d) and 4(e) show maps of the magnetic spectrum as a function of wavevector along $(h, 1-h, 0)$ for energies between 2 meV and 7 meV at 2 and 40 K. At 2 K we find a strong signal in $\chi''(\boldsymbol{Q}, E)$ centred on $\boldsymbol{Q} = (1/2, 1/2, 0)$ and $E \sim 7$ meV. This feature corresponds to the spin resonance reported previously in superconducting $FeSe_{0.4}Te_{0.6}$ [16], $FeSe_{0.46}Te_{0.54}$ [18] and $FeSe_{0.5}Te_{0.5}$ [19]. At higher energies, the excitations have been found to disperse away from $(1/2, 1/2, 0)$ along $(1, -1, 0)$ [18]. However, it is the low energy response of the system which shows the most dramatic change on transition into the superconducting state, as may be seen in figure 4(f). As the sample is cooled from 40 K to 2 K, the integrated dynamical susceptibility of the peak at 7 meV increases by more than a factor of 2 and decreases in width along $(1, -1, 0)$ by $\sim 30\%$. Fluctuations continue to be observed well above T_c.

4. Discussion

In combination with earlier measurements, the results presented here establish that the low-energy magnetic dynamics of $Fe_{1+y}Se_xTe_{1-x}$ vary strongly with x. The

magnetic spectra of the magnetically-ordered compound ($x = 0.25$) and the bulk superconductor ($x = 0.5$) both contain low-energy magnetic fluctuations in the vicinity of the antiferromagnetic wavevector $(1/2, 1/2, 0)$. However, at $x = 0.25$ the fluctuations are incommensurate with wavevector $(1/2 \pm \epsilon, 1/2 \mp \epsilon, 0)$, $\epsilon \approx 0.18$, whereas at $x = 0.5$ the strongest magnetic signal is commensurate. Moreover, at $x = 0.5$ the magnetic spectrum has a gap of $\sim 6\,\mathrm{meV}$ and the size of the signal just above the gap increases strongly at low temperatures. This behaviour is consistent with the superconductivity-induced spin resonance reported recently in bulk superconducting samples of $Fe_{1+y}Se_xTe_{1-x}$ of similar composition to ours [16, 17, 18, 19], and also in related Fe pnictide superconductors [26, 27, 28, 29, 30].

A further difference is that the $x = 0.25$ sample exhibits short-range, static (within the μSR time window) magnetic order with a characteristic wavevector $\boldsymbol{q} = (1/2 - \delta, 0, \pm 1/2)$, $\delta \approx 0.03$, whereas according to our μSR data there is no static magnetic order in the bulk superconductor. The magnetic ordering wavevector $\boldsymbol{q}$ found at $x = 0.25$ is the same as that in the parent phase $Fe_{1+y}Te$. The slight incommensurability is thought to be caused by the small excess of Fe accommodated in interstitial sites in the crystal structure [8, 31, 32], although it is interesting that the incommensurability is the same to within experimental error at $y = 0.10$ (the present sample) and at $y = 0.03$ (the sample studied by us previously [11]).

Our results suggest that there are two distinct magnetic ordering tendencies at $x = 0.25$, one with wavevector $(1/2 - \delta, 0, \pm 1/2)$ and the other with wavevector $(1/2 \pm \epsilon, 1/2 \mp \epsilon, 0)$. The μSR data indicate that the volume fraction of magnetically ordered phase is close to 100%, but we cannot say whether the two characteristic magnetic correlations coexist on an atomic scale or whether the sample is magnetically inhomogeneous.

Finally, we comment on the fact that in the $x = 0.25$ sample diffuse peaks are observed in the elastic (within energy resolution) channel below $T \approx 50\,\mathrm{K}$ by neutron scattering but static magnetic order is only detected below $T \approx 35\,\mathrm{K}$ by μSR. These observations can be reconciled by the difference in the fluctuation rates observable by muons ($\sim$ GHz) and neutrons ($\sim$ THz) below which spin freezing is measured. We infer from this that the characteristic fluctuations of the spin system lie between $\sim$GHz and $\sim$THz for $35\,\mathrm{K} \lesssim T \lesssim 50\,\mathrm{K}$. Such a gradual slowing down of the fluctuations could be a consequence of the quasi-two-dimensional nature of the spin system, which is also indicated by the persistence of spin correlations to temperatures well above the ordered phase. It is also interesting that the size of the magnetically ordered domains does not significantly increase with decreasing temperature, which suggests that the short-range order is never truly static but fluctuates down to the lowest temperature investigated. This picture is consistent with the recent observation of spin-glass behaviour in $Fe_{1.1}Se_xTe_{1-x}$ for $0.05 < x < 0.55$ [33].

5. Conclusion

We have observed a resonance-like peak at the antiferromagnetic wavevector $(1/2, 1/2, 0)$ in the low-energy magnetic spectrum of $Fe_{1.01}Se_{0.50}Te_{0.50}$, and shown that this feature is absent from the magnetic spectrum of $Fe_{1.10}Se_{0.25}Te_{0.75}$ which instead shows incommensurate peaks flanking $(1/2, 1/2, 0)$. Our results reveal a clear distinction between the magnetic excitation spectra of $Fe_{1+y}Se_xTe_{1-x}$ samples which are magnetically ordered and those which are bulk superconductors. We conclude that the existence of a resonance peak at the commensurate antiferromagnetic wavevector is a characteristic of bulk superconductivity in $Fe_{1+y}Se_xTe_{1-x}$.

Acknowledgments

This work was performed at the Paul Scherrer Institut, Villigen, Switzerland. P.B. is grateful for the provision of a studentship from the U.K. Engineering and Physical Sciences Research Council.

References

[1] K. Ishida, Y. Nakai, and H. Hosono. *J. Phys. Soc. Japan*, 78(6):062001, 2009.
[2] J. W. Lynn and P. Dai. *Physica C*, 469(9-12):469–476, 2009.
[3] M. R. Norman. *Phys.*, 1:21, 2008.
[4] B. C. Sales, A. S. Sefat, M. A. McGuire, R. Y. Jin, D. Mandrus, and Y. Mozharivskyj. *Phys. Rev. B*, 79(9):094521–5, 2009.
[5] G. F. Chen, Z. G. Chen, J. Dong, W. Z. Hu, G. Li, X. D. Zhang, P. Zheng, J. L. Luo, and N. L. Wang. *Phys. Rev. B*, 79(14):140509–4, 2009.
[6] F.-C. Hsu, J.-Y. Luo, K.-W. Yeh, T.-K. Chen, T.-W. Huang, P. M. Wu, Y.-C. Lee, Y.-L. Huang, Y.-Y. Chu, D.-C. Yan, and M.-K. Wu. *Proc. Natl. Acad. Sci.*, 105(38):14262–14264, 2008.
[7] F. Grønvold, H. Haraldsen, and J. Vihovde. *Acta Chem. Scand.*, 8:1927–1942, 1954.
[8] W. Bao, Y. Qiu, Q. Huang, M. A. Green, P. Zajdel, M. R. Fitzsimmons, M. Zhernenkov, S. Chang, M. H. Fang, B. Qian, E. K. Vehstedt, J. H. Yang, H. M. Pham, L. Spinu, and Z. Q. Mao. *Phys. Rev. Lett.* , 102(24):247001, 2009.
[9] K. W. Yeh, C. T. Ke, T. W. Huang, T. K. Chen, Y. L. Huang, P. M. Wu, and M. K. Wu. *Cryst. Growth Des.*, 9(11):4847–4851, 2009.
[10] M. H. Fang, H. M. Pham, B. Qian, T. J. Liu, E. K. Vehstedt, Y. Liu, L. Spinu, and Z. Q. Mao. *Phys. Rev. B*, 78(22):224503, 2008.
[11] R. Khasanov, M. Bendele, A. Amato, P. Babkevich, A. T. Boothroyd, A. Cervellino, K. Conder, S. N. Gvasaliya, H. Keller, H. H. Klauss, H. Luetkens, V. Pomjakushin, E. Pomjakushina, and B. Roessli. *Phys. Rev. B*, 80(14):140511–4, 2009.
[12] S. Margadonna, Y. Takabayashi, Y. Ohishi, Y. Mizuguchi, Y. Takano, T. Kagayama, T. Nakagawa, M. Takata, and K. Prassides. *Phys. Rev. B*, 80(6):064506, 2009.
[13] Y. Mizuguchi, F. Tomioka, S. Tsuda, T. Yamaguchi, and Y. Takano. *Appl. Phys. Lett.*, 93(15):152505–3, 2008.
[14] S. Medvedev, T. M. McQueen, I. A. Troyan, T. Palasyuk, M. I. Eremets, R. J. Cava, S. Naghavi, F. Casper, V. Ksenofontov, G. Wortmann, and C. Felser. *Nat. Mater.*, 8(8):630–633, 2009.
[15] G. Garbarino, A. Sow, P. Lejay, A. Sulpice, P. Toulemonde, M. Mezouar, and M. Nunez-Regueiro. *Europhys. Lett.*, 86(2):27001, 2009.

[16] Y. Qiu, W. Bao, Y. Zhao, C. Broholm, V. Stanev, Z. Tesanovic, Y. C. Gasparovic, S. Chang, J. Hu, B. Qian, M. H. Fang, and Z. Q. Mao. *Phys. Rev. Lett.* , 103(6):067008–4, 2009.

[17] S. Iikubo, M. Fujita, S. Niitaka, and H. Takagi. *J. Phys. Soc. Japan* , 78(10):103704, 2009.

[18] D.N. Argyriou, A. Hiess, A. Akbari, I. Eremin, M.M. Korshunov, J. Hu, B. Qian, Z. Q. Mao, Y. Qiu, C. Broholm, and W. Bao. *arXiv:0911.4713v1*, 2009.

[19] H. A. Mook, M. D. Lumsden, A. D. Christianson, S. E. Nagler, B. C. Sales, R. Jin, M. A. McGuire, A. S. Sefat, D. Mandrus, T. Egami, and C. de la Cruz. *arXiv:0911.5463v2*, 2009.

[20] F. Semadeni, B. Roessli, and P. Böni. *Physica B*, 297(1-4):152–154, 2001.

[21] W. E. Fischer. *Physica B*, 234-236:1202–1208, 1997.

[22] R. Khasanov, K. Conder, E. Pomjakushina, A. Amato, C. Baines, Z. Bukowski, J. Karpinski, S. Katrych, H. H. Klauss, H. Luetkens, A. Shengelaya, and N. D. Zhigadlo. *Phys. Rev. B*, 78(22):220510, 2008.

[23] J. Wen, G. Xu, Z. Xu, Z. W. Lin, Q. Li, W. Ratcliff, G. Gu, and J. M. Tranquada. *Phys. Rev. B*, 80(10):104506–4, 2009.

[24] G. Shirane. *Neutron scattering with a triple-axis spectrometer: basic techniques*. Cambridge: Cambridge University Press, 2002.

[25] M. D. Lumsden, A. D. Christianson, E. A. Goremychkin, S. E. Nagler, H. A. Mook, M. B. Stone, D. L. Abernathy, T. Guidi, G. J. MacDougall, C. de la Cruz, A. S. Sefat, M. A. McGuire, B. C. Sales, and D. Mandrus. *Nat. Phys.*, 6:182–186, 2010.

[26] A. D. Christianson, E. A. Goremychkin, R. Osborn, S. Rosenkranz, M. D. Lumsden, C. D. Malliakas, I. S. Todorov, H. Claus, D. Y. Chung, M. G. Kanatzidis, R. I. Bewley, and T. Guidi. *Nature*, 456(7224):930–932, 2008.

[27] M. D. Lumsden, A. D. Christianson, D. Parshall, M. B. Stone, S. E. Nagler, G. J. MacDougall, H. A. Mook, K. Lokshin, T. Egami, D. L. Abernathy, E. A. Goremychkin, R. Osborn, M. A. McGuire, A. S. Sefat, R. Jin, B. C. Sales, and D. Mandrus. *Phys. Rev. Lett.* , 102(10):107005, 2009.

[28] S. Chi, A. Schneidewind, J. Zhao, L. W. Harriger, L. Li, Y. Luo, G. Cao, Z. Xu, M. Loewenhaupt, J. Hu, and P. Dai. *Phys. Rev. Lett.* , 102(10):107006, 2009.

[29] S. Li, Y. Chen, S. Chang, J. W. Lynn, L. Li, Y. Luo, G. Cao, Z. Xu, and P. Dai. *Phys. Rev. B*, 79(17):174527, 2009.

[30] D. S. Inosov, J. T. Park, P. Bourges, D. L. Sun, Y. Sidis, A. Schneidewind, K. Hradil, D. Haug, C. T. Lin, B. Keimer, and V. Hinkov. *Nat. Phys.*, 6:178–181, 2010.

[31] C. Fang, B. A. Bernevig, and J. Hu. *Europhys. Lett.*, 86(6):67005, 2009.

[32] F. Ma, W. Ji, J. Hu, Z.-Y. Lu, and T. Xiang. *Phys. Rev. Lett.* , 102(17):177003–4, 2009.

[33] P. L. Paulose, C. S. Yadav, and K. M. Subhedar. *arXiv:0907.3513v1*, 2009.